African Journal of Biotechnology Vol. 7 (6), pp. 689-695, 18 March, 2008
Available online at http://www.academicjournals.org/AJB
ISSN 1684–5315 © 2008 Academic Journals

Full Length Research Paper

Viscoelastic finite-element analysis of human skull - dura mater system as intracranial pressure changing

Xianfang Yue*, Li Wang, Shufeng Sun, Lige Tong

School of Mechanical Engineering, University of Science and Technology Beijing, Beijing 100083, China.

Accepted 18 January, 2008

In the work, the dynamic characteristics of the human skull-dura mater system were studied. For the purpose of our analysis, we adopted a model consisted of a hollow sphere. By using the 'Patran and Ansys' finite element processor, a simplified three-dimensional finite element model (FEM) of a human skull was constructed. The model was used to calculate the deformation of human skull with the intracranial pressure changing. This required good representation of the complex anatomy of the skull. Four different entities are distinguished: Tabula externa, Tabula interna, and a porous Diploe sandwiched in between, and dura mater. A thin-walled skull was simulated by composite shell elements. The viscoelasticity of human skull-dura mater system was studied and analyzed by the finite-element Maxwell model. The 1/8 model consisted of 25224 nodes and 24150 three-dimensional 8-node isoparametric solid elements. The elastic-viscous mechanical characteristics must be used for the skull. The viscous strains account for about 40% of total strains of human skull and dura mater. And the range of strain errors is from 6.45 to 14.82% after ignoring the viscosity of skull and dura mater.

Key words: Viscoelasticity, finite-element analysis (FEA), strain, human skull, dura mater, intracranial pressure.

INTRODUCTION

Intracranial pressure (ICP) is the pressure exerted by the brain, cerebrospinal fluid (CSF), and the brain's blood supply on closed intracranial space. One of the most damaging aspects of brain trauma and other conditions, directly correlated with poor outcome, is an elevated ICP (Orlando, 2004). An increase in normal brain pressure can be due to an increase in CSF pressure. It can also be due to increased pressure within the brain matter caused by lesions or swelling within the brain matter itself. Raised ICP is often not preventable. The pressure itself can be responsible for further damage to the central nervous system by causing compression of important brain structures and by restricting blood flow through blood vessels that supply the brain. Raised ICP is a serious and often fatal condition. ICP cannot go past 40 mmHg in an adult without causing severe harm (Dawodu, 2004). Even ICPs between 25 and 30 mmHg are usually fatal if prolonged, except in children, who can tolerate higher pressures for longer times (Tolias and Sgouros, 2003). Compression of vital brain structures and blood vessels can lead to serious, permanent neurologic deficits or even death.

The 'Monro (1823) - Kellie (1824) doctrine' states that an adult cranial compartment is incompressible, and the volume inside the cranium is a fixed volume thus creates a state of volume equilibrium, such that any increase of the volumes of one component (i.e. blood, CSF, or brain tissue) must be compensated by a decrease in the volume of another. If this cannot be achieved then pressure will rise and once the compliance of the intracranial space is exhausted then small changes in volume can lead to potentially lethal increases in ICP. The compensatory mechanism for intracranial space occupation obviously has limits. When the amount of CSF and venous blood that can be extruded from the skull has been exhausted, the ICP becomes unstable and waves of pressure develop (Lundberg, 1960). As the process of space occupation continues, the ICP can rise to very high levels and the brain can become displaced from its normal position. Dr. Sutherland (1939) first perceived a subtle palpable movement within the bones of cranium. Dr. Upledger (Retzlaff et al., 1973) discovered that the inherent rhythmic motion of cranial bones was caused by the fluctuation of CSF. Accordingly, the cranium can move and be deformed as the ICP fluctuates.

The craniospinal cavity may be considered as a ball-

*Corresponding author. E-mail: yuexf@me.ustb.edu.cn. Tel: +86-01-62334994. Fax: +86-10-62329145.

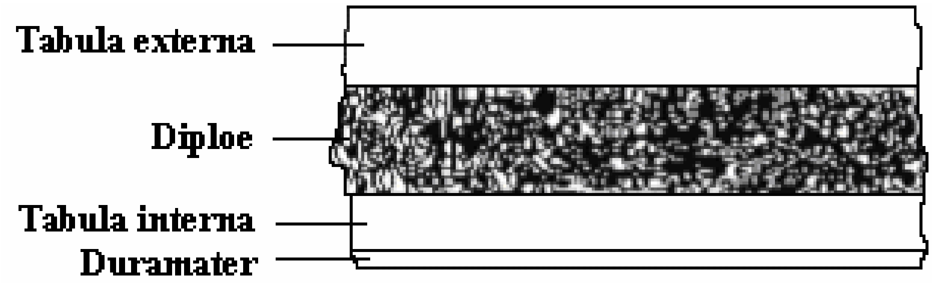

Figure 1. Sketch of layered sphere. The thin-walled structure of cranial cavity is mainly composed of Tabula externa, Diploe, Tabula interna and dura mater.

Table 1. Strains of ignoring the viscoelasticity of human skull and dura mater with the increasing intracranial pressure (ICP).

ICP variation (kPa)	1.5	2.0	2.5	3.0	3.5	4.0	4.5	5.0
Strains(με)	1.002	1.13	1.55	2.35	2.86	3.18	3.57	3.98

oon. For the purpose of our analysis, we adopted the model of hollow sphere. We presented the development and validation of a 3D finite-element model intended to better understand the deformation mechanisms of human skull corresponding to the ICP change. The skull is a layered sphere constructed in a specially designed form with a Tabula externa, Tabula interna, and a porous Diploe sandwiched in between. Based on the established knowledge of cranial cavity importantly composed of skull and dura mater (Figure 1), a thin-walled structure is simulated by the composite shell elements of the finite-element software (Piekarshi, 1973). The important mechanical characteristic of cancellous bone and dura mater is viscoelasticity (Odgaard, 1997; Noort et al., 1981).

MATERIALS AND METHODS

In order to determine the influence of the viscoelastic nature of the human skull and dura mater on their deformation, we made the finite-element analysis of cranial cavity with the ICP scope from 1.5 to 5 kPa respectively. By ignoring the viscoelasticity of human skull and dura mater, the initial FEM of skull-dura mater system was carried out. With the viscoelasticity of human skull and dura mater, using the second FEM, the displacements of skull-dura mater system were calculated.

In this work, the finite-element software MSC_PATRAN/NASTRAN and ANSYS were applied to theoretically analyze the deformation of human skull with the changing ICP. The external diameter of cranial cavity is about 200 mm. The thickness of shell is the mean thickness of calvarias. The average thickness of adult's calvaria is 6.0 mm, that of Tabula externa is 2.0 mm, diploe is 2.8 mm, Tabula interna is 1.2 mm and, dura mater in the parietal position is 0.4 mm.

FEA of strains by ignoring the viscoelasticity of human skull and dura mater

By ignoring the viscoelasticity of human skull and dura mater, we first simplified the theoretical model. The deformation of human skull was analyzed with the finite-element software MSC_PATRAN/NASTRAN. Considering the characteristic of compact bone, cancellous bone and dura mater, we adopted their elastic modulus and Poisson ratios as 1.5×10^4 MPa, 4.5×10^3 MPa (Willinger et al., 1999), 1.3×10^2 MPa (Ding et al., 1998) and 0.21, 0.01, 0.23 respectively.

After ignoring the viscoelasticity of human skull and dura mater, the strains of cranial cavity are shown in Table 1 with the finite-element software MSC_PATRAN/NASTRAN as ICP changing from 1.5 to 5.0 kPa. There is measurable correspondence between skull strains and ICP variation. The strains of human skull could reflect the ICP change. When ICP variation was raised up to 2.5 kPa, the stress and strain graphs of skull bone are shown in Figure 2.

FEA of strains by considering the viscoelasticity of human skull - dura mater system

Under the constant action of stress, the strain of ideal elastic solid is invariable and that of ideal viscous fluid keeps on growing at the equal ratio with time. However, the strain of actual material increases with time, namely so-called creep. Generally, Maxwell and Kelvin models are the basic models to describe the performance of viscoelastic materials. Maxwell model represents in essence the liquid. Despite the representative of solid, Kelvin model cannot describe stress relaxation but only stress creep. So the combined models made up of the primary elements are usually adopted to describe the viscoelastic performance of actual materials. The creep of linear viscoelastic solid can be simulated by the Kelvin model of three parameters or the generalized Kelvin model.

Viscoelastic model of human skull

Kelvin model of three parameters is shown in Figure 3 (a). Figure 3 (b) shows the relaxation curves of human skull and Kelvin model of three parameters in the compressive experiment. Figure 3(c) depicts the creep curves of human skull and Kelvin model of three parameters. It showed that the theoretical Kelvin model of three parameters could well simulate the mechanical properties of human skull in the tensile experiments. Thus the Kelvin model of three parameters was adopted to describe the viscoelasticity of human skull in this paper.

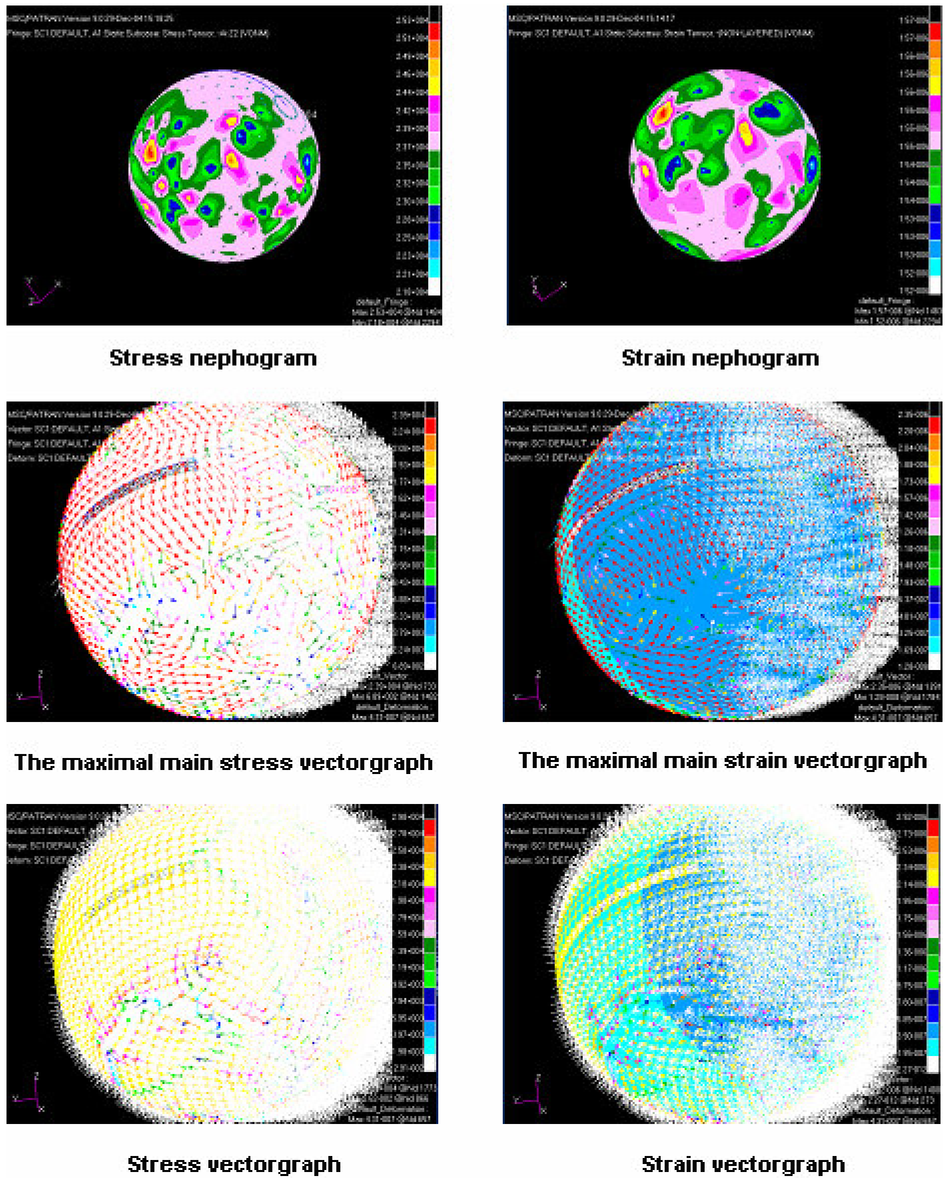

Figure 2. Stress and strain graphs of cranial cavity by ignoring the viscoelasticity of human skull and dura mater with finite-element software MSC_ PATRAN/NASTRAN when ICP variation is raised up to 2.5 kPa.

For the Kelvin model of three parameters, the stress and strain of human skull are shown in equation (1),

$$\begin{cases} \varepsilon = \varepsilon_0 + \varepsilon_1 \\ \sigma = E_1\varepsilon_1 + \eta\dot{\varepsilon}_1 \\ \sigma = E_0\varepsilon_0 \end{cases} \tag{1}$$

After the calculation based on the equation (1), the elastic modulus of human skull is shown in equation (2),

$$E = \left(\frac{E_0E_1}{E_0+E_1}\right) + \left(\frac{E_0^2}{E_0+E_1}\right)e^{\frac{t}{P_1}} \tag{2}$$

Here, σ, Direct stress acted on elastic spring or impact stress acted on viscopot; ε, Direct strain of elastic spring; E, Elastic modulus of tensile compression; η, Viscosity coefficient of viscopot; $\dot{\varepsilon}$, strain ratio;

$$P_1 = \frac{\eta}{E_0 + E_1}$$

Viscoelastic model of human dura mater

The generalized Kelvin model is shown in Figure 3 (d). Figure 3 (e) is the creep experimental curves of human dura mater. Figure 3 (f)

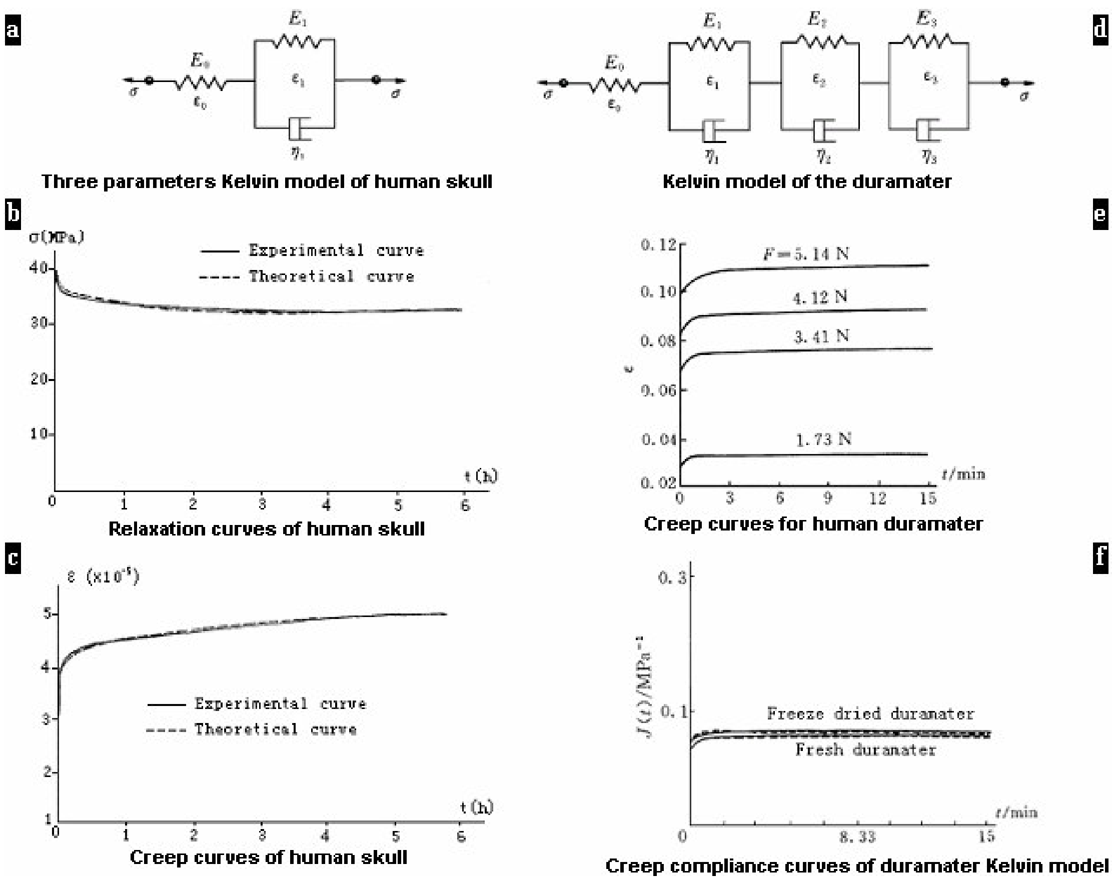

Figure 3. Viscoelastic Kelvin model of human skull and dura mater. a. Three-parameters Kelvin model of human skull. b. Relaxation train-time curves of the experiment and three-parameters Kelvin theoretical model for human skull. c. Creep train-time curves of the experiment and three-parameters Kelvin theoretical model for human skull. d. Generalized Kelvin model of the human dura mater. e. Creep train-time curves under different actions for fresh human dura mater (L_0 = 23 mm, θ = 37^0). f. Creep compliance curves of generalized Kelvin model for human dura mater.

shows the curves of creep compliance for the generalized Kelvin model. It shows that the tendency of creep curve in the experiment is coincident with that of creep compliance for the generalized Kelvin model. Creep is the change law of material deformation with time under the invariable stress, so here σ is constant. For the generalized Kelvin model, the stress-strain relationship is $\varepsilon(t) = J(t)\sigma$. Thus the tendency of theoretical creep curve is totally the same as that of experimental one for human dura mater. So in this paper, the generalized Kelvin model composed of three Kelvin-unit chains and a spring was adopted to simulate the viscoelasticity of human dura mater in this paper.

For the viscoelastic model of human dura mater composed of the three Kelvin-unit chains and a spring, the stress and strain of human dura mater are shown in equation (3),

$$\begin{cases} \varepsilon = \varepsilon_0 + \varepsilon_1 + \varepsilon_2 + \varepsilon_3 \\ \varepsilon_0 = \dfrac{\sigma}{E_0} \\ \sigma = E_1\varepsilon_1 + \eta_1\dot{\varepsilon}_1 = E_2\varepsilon_2 + \eta_2\dot{\varepsilon}_2 = E_3\varepsilon_3 + \eta_3\dot{\varepsilon}_3 \end{cases} \quad 3$$

After the calculation based on the equation (3), the creep compliance of human dura mater is presented in equation (4),

$$J(t) = E_0^{-1} + E(1 - \mathrm{e}^{-t/\tau_1}) + E_2^{-1}(1 - \mathrm{e}^{-t/\tau_2}) + E_3^{-1}(1 - \mathrm{e}^{-t/\tau_3}) \quad 4$$

Then the elastic modulus of human dura mater is shown in equation (5),

$$E = \left[E_0^{-1} + E_1^{-1}\left(1 - \mathrm{e}^{-t/\tau_1}\right) + E_2^{-1}\left(1 - \mathrm{e}^{-t/\tau_2}\right) + E_3^{-1}\left(1 - \mathrm{e}^{-t/\tau_3}\right)\right]^{-1} \quad 5$$

Here, σ, ε, E, η, $\dot{\varepsilon}$ is Ditto mark; τ_1, τ_2, τ_3 is lag time, that is $\tau_1 = \eta_1 / E_1$, $\tau_2 = \eta_2 / E_2$, $\tau_3 = \eta_3 / E_3$.

In the finite-element software ANSYS, there are three kinds of models to describe the viscoelasticity of actual materials, in which the Maxwell model is the general designation for the combined Kelvin and Maxwell models. Considering the mechanical properties of human skull and dura mater, we adopted the finite-element Maxwell model to simulate the viscoelasticity of human skull-dura mater system. The viscoelastic parameters of human skull and dura mater are respectively listed in Tables 2 and 3.

The three-dimensional stress-strain relationships for a linear isotropic viscoelastic material are given by:

Table 2. Coefficients for the viscoelastic properties for human skull.

Parameter	Elastic Modulus(GPa)		Viscosity(GPa/s)		Delay time(s)
	E_0	E_1	η	τ_γ^*	τ_d^*
Compression	5.69±0.26	42.24±2.09	96840±5400	2022±198	2292±246
Tension	13.64±0.59	51.45±2.54	206100±15360	3180±300	4026±372

$^*\tau_r = \eta / (E_0+E_1), \tau_d = \eta / E_1$

Table 3. Creep coefficients for the viscoelastic properties for fresh human dura mater.

Parameter	Elastic modulus(MPa)				Delay time(s)		
	E_0	E_1	E_2	E_3	τ_1	τ_2	τ_3
dura mater	16.67	125.0	150.0	93.75	40	10^4	10^6

$$\sigma_{ij} = \int_0^t \left[2G(t-\tau)\frac{\partial e_{ij}(\tau)}{\partial \tau} + \delta_{ij} K(t-\tau)\frac{\partial \theta(\tau)}{\partial \tau} \right] d\tau ;\quad i, j = 1,2,3 \qquad 6$$

Here σ_{ij}, the Cauchy stress tensor; e_{ij}, the deviatoric strain tensor; δ_{ij}, the Kronecker delta; $G(t)$, the shear relaxation function; $K(t)$, the bulk relaxation function; $\theta(t)$, the volumetric strain; t, the present time; τ, the past time.

Human skull has the viscoelastic material (Charalambopoulos et al., 1998). Considering the viscoelasticity of human skull and dura mater, we used the viscoelastic option of the ANSYS finite-element program to analyze the strains on the exterior surface of human skull as ICP changing. According to the symmetry of 3D model of human skull, the preprocessor of the ANSYS finite-element program was used to construct a 1/8 finite-element model of human skull and dura mater consisting of 25224 nodes and 24150 three-dimensional 8-node isoparametric solid elements, shown in Figure 4 (f).

RESULTS AND DISCUSSION

Under the same loading conditions, the results were compared with the initial FEM. Figure 4 (a) ~ (e) are the analytic graphs of stress and strain with finite-element software ANSYS when ICP variation was raised up to 2.5 kPa. It shows that the stress and strain distributions on the exterior surface of human skull are well-proportioned and that the stress and strain variations on the exterior surface of cranial cavity are relatively small corresponding to the ICP change.

The relationships about total, elastic and viscous strains of human skull and dura mater are shown in Figure 4 (g). The strains of cranial cavity are shown in Figure 5 separately by ignoring and considering the viscoelasticity of human skull and dura mater with the changing ICP. An alternative methodology, to treat viscoelastic problems, dynamic or not, by FEMs has been proposed and successfully implemented. This new methodology considers the viscosity characteristics of cranial cavity. From the results obtained we can conclude that there is a big influence of the viscoelastic nature of the human skull and dura mater material on their deformation.

According to the mechanism of mechanical deformation, human skull and dura mater becomes deformed as the ICP changes. The strains of cranial cavity are coincident with ICP variation. The deformation scope of human skull is theoretically from 0.9 to 3.4 $\mu\varepsilon$ as the ICP changing from 1.5 to 5.0 kPa. Corresponding to ICP of 2.5, 3.5 and 5.0 kPa, the strain of skull deformation separately for mild, moderate and severe head injury is 1.5, 2.4, and 3.4 $\mu\varepsilon$ or so. The viscous strains accounted for about 40% of total strains of human skull and dura mater with the changing ICP. The error range of cranial cavity strain is from 6.45 to 14.82% after ignoring the viscosity of human skull and dura mater.

The elastic-viscous mechanical characteristics must be used for the skull. The viscoelasticity of human skull and dura mater has a greater influence on the deformation and strains of cranial cavity as the ICP changing. The viscoelastic nature of human skull and dura mater can influence the human's health. Therefore, the material significance of cranial cavity is very important.

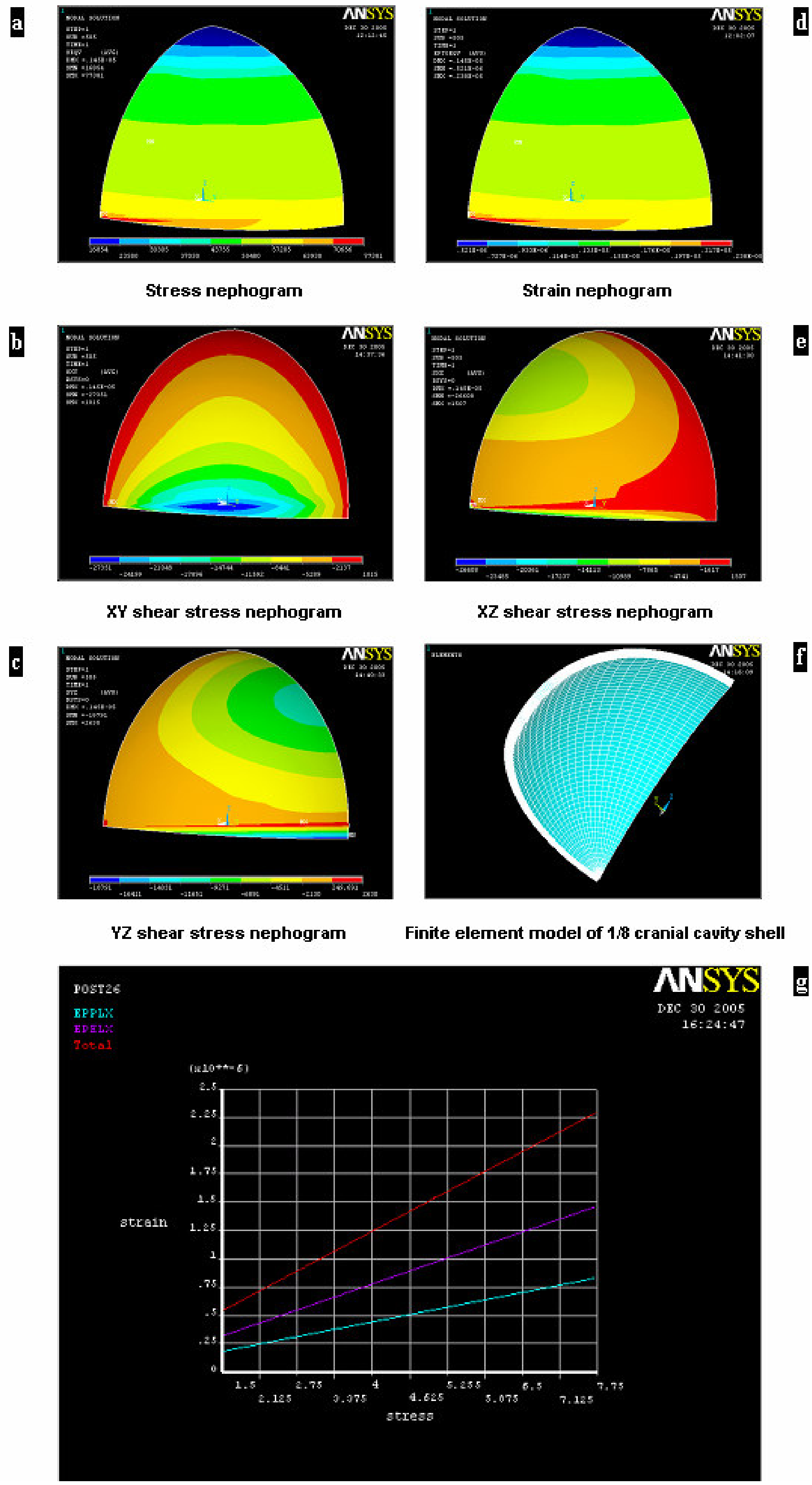

Figure 4. FEA of strains of cranial cavity by considering the viscoelasticity of human skull and dura mater with finite-element software ANSYS when the ICP increment is 2.5 kPa. a. Stress graph. b. Strain graph. c, XY shear stress graph. d. XZ shear stress graph. e. YZ shear stress graph. f. Finite-element model of 1/8 cranial cavity shell. g. Relationship curves about total, elastic and viscous strains of cranial cavity. Here EPELX is the elastic strain curve and EPPLX is the viscous strain curve. The viscous strains are about 40% of total strains.

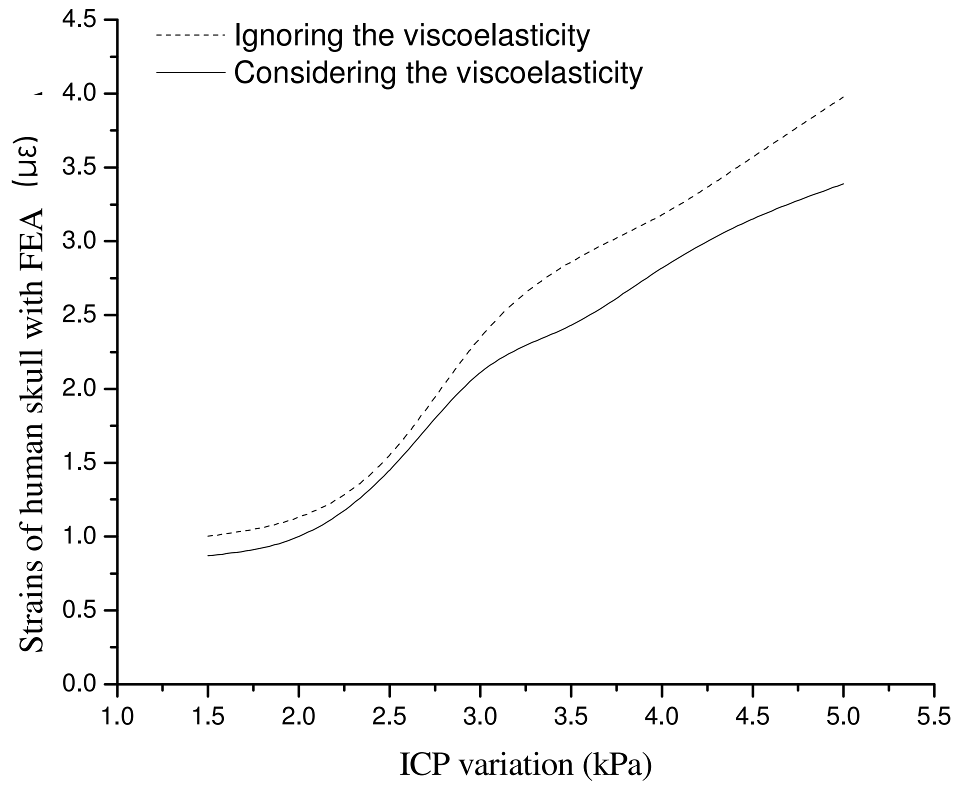

Figure 5. The strains of cranial cavity by respectively ignoring and considering the viscoelasticity of human skull and dura mater with the finite-element software MSC_ PATRAN/NASTRAN and ANSYS with the changing ICP from 1.5 to 5 kPa.

REFERENCES

Charalambopoulos A, Fotiadis DI, Massalas CV (1998). Free vibrations of the viscoelastic human skull. Int. J. Eng. Sci. 36 (5-6): 565-576.

Dawodu S (2004). Traumatic Brain Injury: Definition, Epidemiology, Pathophysiology. Emedicine.com.

Ding ZR, Song DL, Li SQ, Zhou LF (1998). Creep behaviour of dura and substitutes. J. Shanghai JiaoTong University 32: 93-96.

Kellie G (1824). An account of the appearances observed in the dissection of two of the three individuals presumed to have perished in the storm of the 3rd, and whose bodies were discovered in the vicinity of Leith on the morning of the 4th November 1821 with some reflections on the pathology of the brain. Edinburgh: Trans. Med. Chir. Sci. 1: 84-169.

Lundberg N (1960). Continuous recording and control of ventricular fluid pressure in neurosurgical practice. Acta Psychiat. Neurol. Scand. (Suppl) 36: 149.

Monro A (1823). Observations on the structure and function of the nervous system. Edinburgh, Creech & Johnson, p. 5.

Noort van R, Black MM, Martin TR (1981). A study of the uniaxial mechanical properties of human dura mater preserved in glycerol. Biomaterials 2: 41-45.

Odgaard A (1997). Three-dimensional methods for quantification of cancellous bone architecture. Bone 20: 315-328.

Orlando Regional Healthcare (ORH) (2004). Education and Development. Overview of Adult Traumatic Brain Injuries.

Piekarshi K (1973). Analysis of bone as a composite material. Int. J. Eng. Sci. 11: 557-565.

Retzlaff EW, Jones L, Mitchell FL, Upledger J (1973). Possible autonomic innervation of cranial sutures of primates and other animals. Brain Res. 58: 470-477.

Sutherland WG (1939). The cranial bowl. Mankato, Minn: Free Press Company.

Tolias C, Sgouros S (2003). Initial Evaluation and Management of CNS Injury. Emedicine.com.

Willinger R, Kang HS, Diaw BM (1999). Development and validation of a human head mechanical model. Comptes Rendus de l'Academie des Sciences Series IIB Mechanics 327: 125-131.